

Degradation of δ -alumina fibre during extrusion of Al–20Si–X powder metallurgical composite

J. H. TER HAAR, J. DUSZCZYK

Laboratory of Materials Science, Delft University of Technology, Rotterdamseweg 137, 2628 AL, Delft, The Netherlands

Powder metallurgical composites consisting of atomized Al–Si–X powder and Saffil δ -alumina fibres were previously consolidated by hot extrusion using various reduction ratios. The microstructure at the fibre–matrix interface, as well as the fibre chemistry of some of these composites, were investigated. The results point towards a relation between mechanical fibre damage during extrusion, extrusion reduction ratio, fibre volume fraction and matrix solute enrichment of fibres. Arguments are forwarded to support the view that the fibres' specific internal texture (porosity/surface), their chemical surface activity at the temperature of extrusion and mechanical fragmentation, allowed the rapidity of the chemical interaction. The mechanical fibre damage partly arose from abrasion by equally hard silicon particles. The implications are that the strength and reinforcing potential of fibres in composites like these can be greatly reduced.

1. Introduction

Alumina-reinforced aluminium matrix composites belong to the group of metal matrix composites (MMCs) most intensively studied. This is partly due to the availability and relative cheapness of the alumina. Moreover, good chemical and physical compatibility between most of the commercial aluminas and alloyed aluminium matrices exists: a strong bond between the two may be achieved, without too much alteration of characteristic properties of either. In molten metal processing routes, such as pressure infiltration and compo/slurry/stir-casting, the extent of chemical interaction between matrix and reinforcement can, however, vary considerably. Magnesium enrichment of a very thin surface layer of Saffil fibres was observed [1, 2] in composites produced by pressure infiltration, while a magnesium-spinel phase has been detected at the interface in magnesium-containing alloys [3–6] of the latter category. It has been reported that the occurrence of a spinel phase may be advantageous for the strength of the interface between metal and oxide [7]. An excess amount of such a brittle phase at the interface is, however, deleterious to its strength [5]. To explain the magnesium enrichment in Saffil fibre-reinforced Al–Mg, some workers postulated a reaction between magnesium in the matrix and the SiO_2 present in the outer surface of these fibres [2, 3]. However, Cappleman *et al.* convincingly demonstrated [8] that the SiO_2 is not necessarily taking part in a reaction but may be merely a condition for magnesium incorporation. They also stress that limited, very superficial, chemical interaction, on the scale of several atomic layers, may cause a strong interfacial bond.

In molten metal processing of composites, chemical heterogeneity formed by segregation effects during

solidification also forms an important drawback: brittle intermetallic compounds at the fibre interface may serve as crack-initiators thus causing premature fracture [6, 9].

The present study concerns the evaluation of δ -alumina fibre-reinforced aluminium composites which were produced by a powder metallurgical (P/M) method. Mechanical properties and fibre-size distributions of these materials were presented in an earlier paper [10]. The morphology and chemistry of the fibres were investigated while efforts were made to characterize the interface.

2. Experimental procedure

Composites based on the air-atomized Al–20 wt % Si–3 wt % Cu–1 wt % Mg alloy with 4.8, 10.0 and 20.0 nominal vol. % Saffil δ -alumina fibre reinforcement were prepared in an earlier stage by dry powder mixing [11], compaction and degassing. The canned and degassed billets were extruded at 450 °C using flat dies and reduction ratios (ER) of 38:1, 18:1 and 10:1.

The materials were studied by optical microscopy employing a Jena Neophot 30, scanning electron microscopy (SEM) on a Jeol 50A apparatus, and transmission electron microscopy (TEM) on a Philips EM 400. The analytical facility of the TEM (Tracor energy dispersive Auger X-ray analysis, EDAX) as well as a Jeol 733 microprobe (electron probe micro analysis (EPMA): wavelength dispersive (WDS) and energy dispersive (EDS)) were used. Thinning of a sample for TEM was done by argon milling, in a Gatan 600 Dif. ion mill. The sample, cooled with liquid nitrogen was bombarded from two sides at an angle of 15° using an ion current of 0.5 mA at 5 kV.

After 5 h operation, additional thinning was required before some fibres were exposed in sufficiently thinned sections. For TEM observation, the sample was mounted in a beryllium specimen holder. The chemistry at the surface of the fibres in the as-received and extruded condition was studied by X-ray photo-electron spectroscopy (XPS) on a Perkin–Elmer PHI electron spectrometer.

X-ray diffraction using an α_1 Guinier camera (Enraf Nonium FR 552) was applied to extracted fibres of selected composite samples, aiming to identify the phases present. The fibres were extracted by dissolution of the matrix in a 45% NaOH solution. After rinsing, the dispersion was boiled for 5 min and filtrated. The undissolved metallic part of the residue was finally dissolved in concentrated HCl, leaving behind a white powder. The fibre residues thus obtained were also subjected to XPS analysis.

3. Results

The chemistry of the surface layer of virgin fibres as determined by XPS is given in Table I. The data are compared with those of more internal regions of the fibre obtained by EPMA. It appears that the surface of the fibre is enriched in silicon with respect to the bulk, by a factor 3.5.

Observation of longitudinal metallographical sections by optical microscopy revealed contrast from distinct structures in fibres of composites with $V_f = 0.100$ and higher, extruded at a reduction ratio of 38:1. Elongated patches emerging from the fibre surface inwards, reveal the existence of planar features (Fig. 1, arrows marked 1). Patches with a fine-grained texture also occur, often at the outer parts of fibres (Figs 1 and 2). These structures arise from light scattering and reflection at internal surfaces along which cohesion is lost. They are identified as surface flaws. Transecting (normal) cracks or surface defects may be inferred from the patterns of interrupted depth fringes (Fig. 1, arrows marked 2), arising from interference of reflecting and incident rays. Fig. 3 shows the microstructure of a $V_f = 0.100$ composite extruded at 18:1. Internal defects in fibres are much less frequent. In many of the fibres in this material, thickness fringes can be seen, providing indirect evidence for a more perfect surface and internal structure. However, in fibres separated from this material by dissolution of the matrix, normal cracks appear to occur frequently (Fig. 4). Composites extruded at the highest reduction ratio of 38:1 have the highest frequency of fibres with internal defects.

One more remarkable feature is that of crenellated fibre boundaries (Figs 1 and 5). This appearance does

TABLE I Chemical composition (at %) of surface (~ 10 nm) and bulk of Saffil Milled fibre as determined with XPS and EPMA, respectively

	[Al]	[Si]	[O]
Bulk	35.96	5.24	58.80
Surface	41.14	1.49	57.31

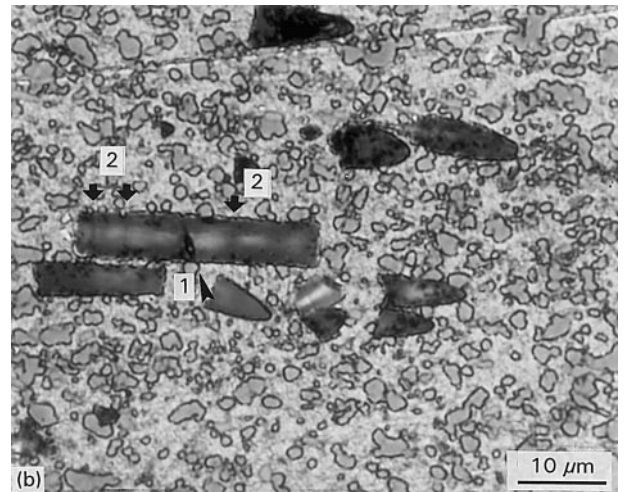
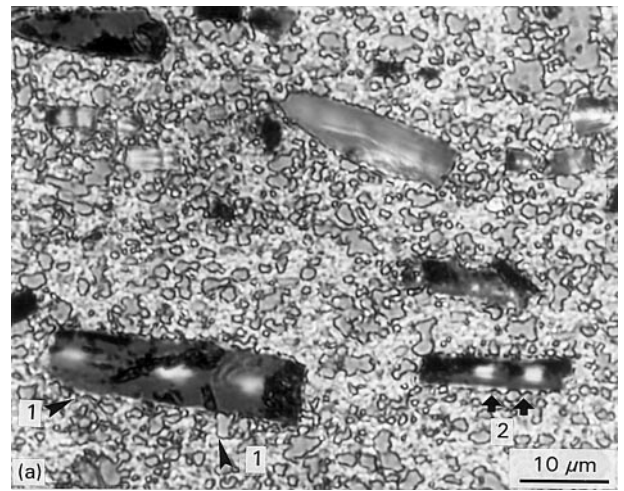


Figure 1 Optical micrographs of a longitudinal sections through composites with $V_f = 0.100/ER$ 38:1 in (a) the as-extruded condition, (b) the T6 heat-treated condition. See text for explanation.

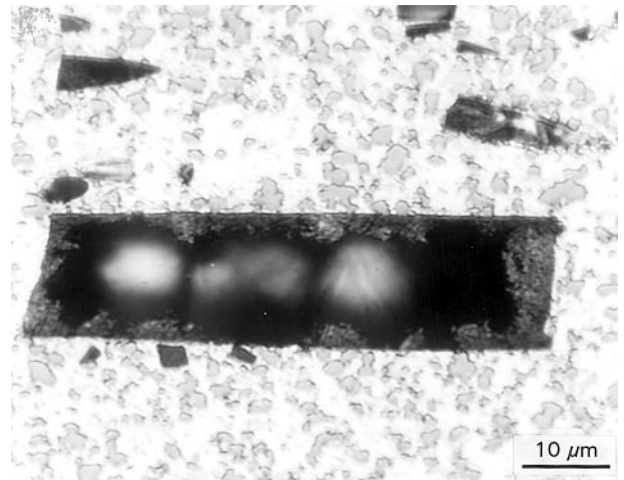


Figure 2 Optical micrograph of a longitudinal section through a composite with $V_f = 0.100/ER$ 38:1, showing a fibre with typical microflaws located at the surface.

not change after a T6 heat treatment consisting of 15 min solution treatment at 495 °C and 4 h ageing at 180 °C (Fig. 1b). Fibres which are originally perfectly circular in cross-section, possess crenellated outlines after extrusion and are clad with small grains of similar relief (Fig. 5). It is relevant to note that fibres

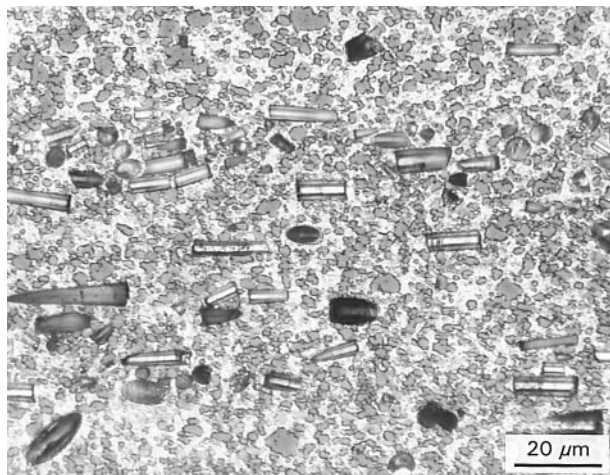


Figure 3 Optical micrograph of a longitudinal section through a composite with $V_f = 0.100/ER\ 18:1$, showing relative damage-free fibres with fringe patterns.

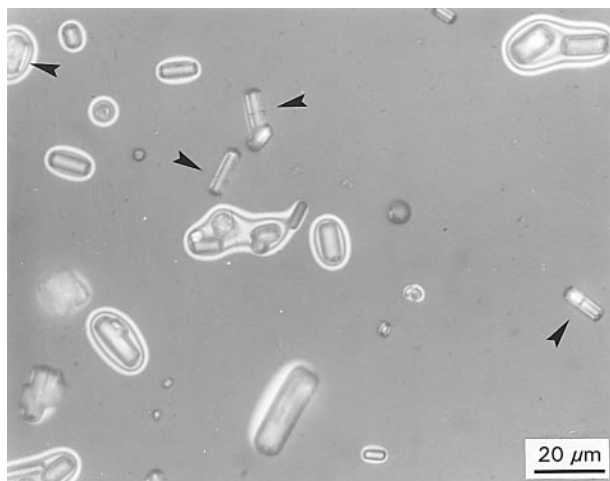


Figure 4 Optical micrograph of fibres dissolved from a composite with $V_f = 0.100/ER\ 18:1$. Fibres display normally transecting cracks (arrows).

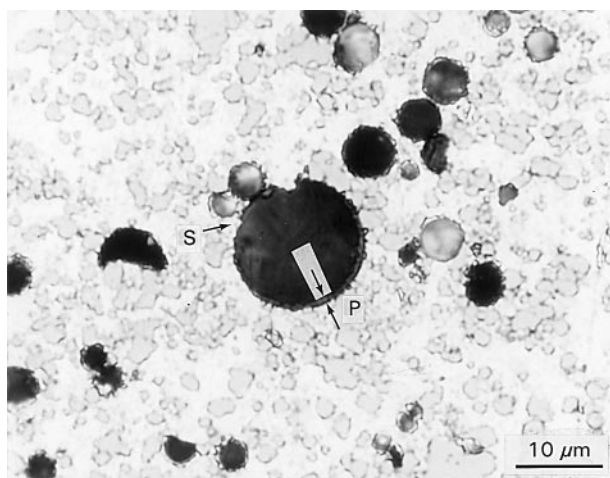


Figure 5 Optical micrograph of a transverse section through a composite with $V_f = 0.100/ER\ 38:1$ in the T6 condition, showing fibres with damaged, abraded surfaces. P, peripheral zone; S, step (see text for explanation).

which are not fully dark in cross-section, contain major defects. Within fibres, a relatively bright peripheral zone with a concentration of fine flaws may be present, representing the same structure as that of the fibre in

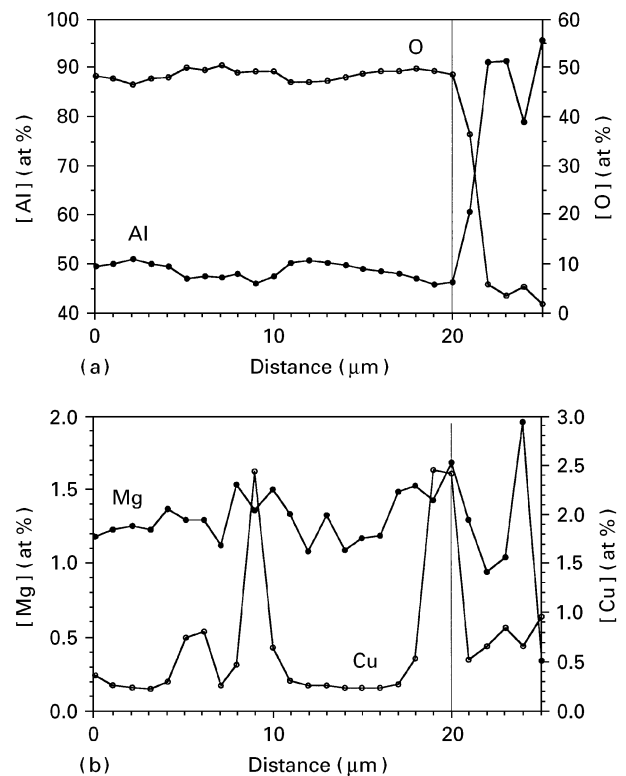


Figure 6 EPMA linescan taken parallel to a fibre, crossing the interface between matrix and fibre end. Composite with $V_f = 0.200/ER\ 38:1$. (a) [Al] and [O], (b) [Mg] and [Cu].

Fig. 2. The width of this cracked peripheral zone varies from zero to a full fibre radius (widely occurring for $V_f = 0.200/38:1$). In the case of the large fibre in Fig. 5, the peripheral zone has a width similar to the size of the cladded grains. Therefore, the grains are likely to represent loose fibres fragments from the cracked peripheral zones. A closer look at this fibre in Fig. 5 indeed reveals a step at the surface (S), separating a fibre segment with a peripheral zone from one where it has been fully eroded.

This implies that fibres can be severely damaged by the extrusion: surface abrasion as well as internal cracking and fragmentation features were demonstrated. This mainly holds for composites with $V_f = 0.100$ and higher and is most severe for materials extruded at the highest reduction ratio of 38:1.

On account of the microstructure in and around the fibres in the present composites, it was decided to check their chemical composition after extrusion. EPMA analyses were performed along traces crossing the interface between fibre and matrix of the $V_f = 0.200$ composite extruded at 38:1. The traces were taken along the fibre axis in longitudinal sections as well as normal to the fibre axis in transverse sections. Analyses along transverse fibre traces on longitudinal composite sections could not be interpreted because the oblique interfaces hold a high risk of irradiating both fibre and matrix.

The results of the quantitative trace analyses are presented in Figs 6 and 7. The minimum outward positions of fibre boundaries in the scan section may be interpreted from the levels of oxygen content and are indicated by vertical lines. While the virgin fibre

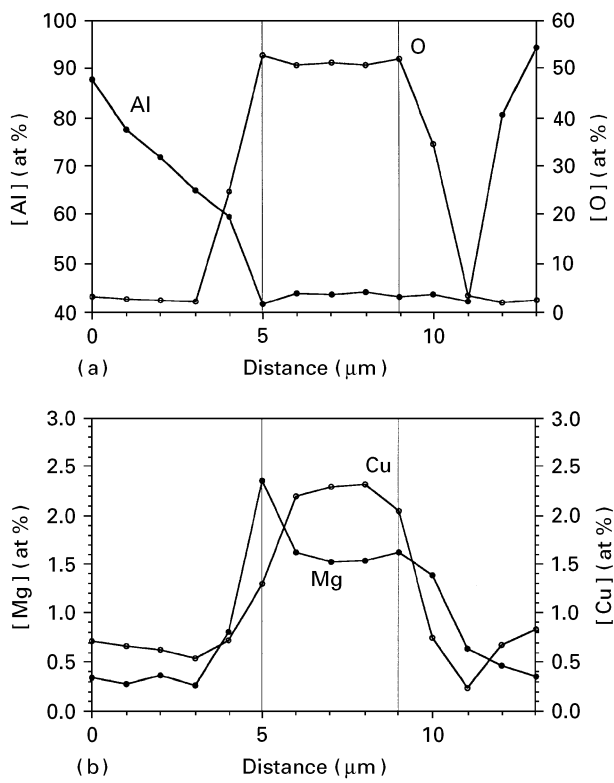


Figure 7 EPMA linescan taken normal to a fibre, on a transverse cross-section of the composite with $V_f = 0.200/\text{ER } 38:1$. (a) [Al] and [O], (b) [Mg] and [Cu].

does not contain significant magnesium (Table I), considerable amounts of this element (in the range 1–1.6 at %) were measured in fibres incorporated in the composite. From one location in the boundary

region of the fibre, a level of 2.4 at % Mg (2.7 wt %) was obtained. Another remarkable feature is the detection of significant amounts of copper in the fibre. The highest level was found at a fibre end close to the interface. It amounted to 2.7 at % Cu (7.7 wt %).

In addition to the EPMA traces, X-ray maps were produced of a transverse section of the same composite. The oxygen and copper maps were produced by the WDS method, while the silicon and magnesium maps were derived by EDS. Fig. 8a–d present the results. In Fig. 8a the BSE image is placed next to the map of oxygen. Fibre contours only scarcely recognized in the former, are much clearer in the latter image. The location of silicon particles is revealed in Fig. 8b. From maps copper and magnesium (Fig. 8c and d), it can be concluded that these elements are not detected in all fibres and that their occurrence is probably not related to the existence of large, nearby magnesium- and copper-rich intermetallics. A remarkable feature is that the highest copper levels are found in the internal regions of fibres whereas those of magnesium preferentially occur in the outer regions.

The interface between fibre and matrix in a relatively undisturbed configuration was studied by TEM. For that purpose, a transversely sectioned sample was prepared of a composite with $V_f = 0.100$ extruded at 18:1. It was rather difficult to find fibres in a sufficiently thin section: their resistance to argon milling is quite large. The metal matrix was found to be in intimate contact with the fibres. In most cases the interface was smooth and circular (Fig. 9a). Fibres possess a grainy internal texture, representing the size of pores and crystallites. The pore channels observed

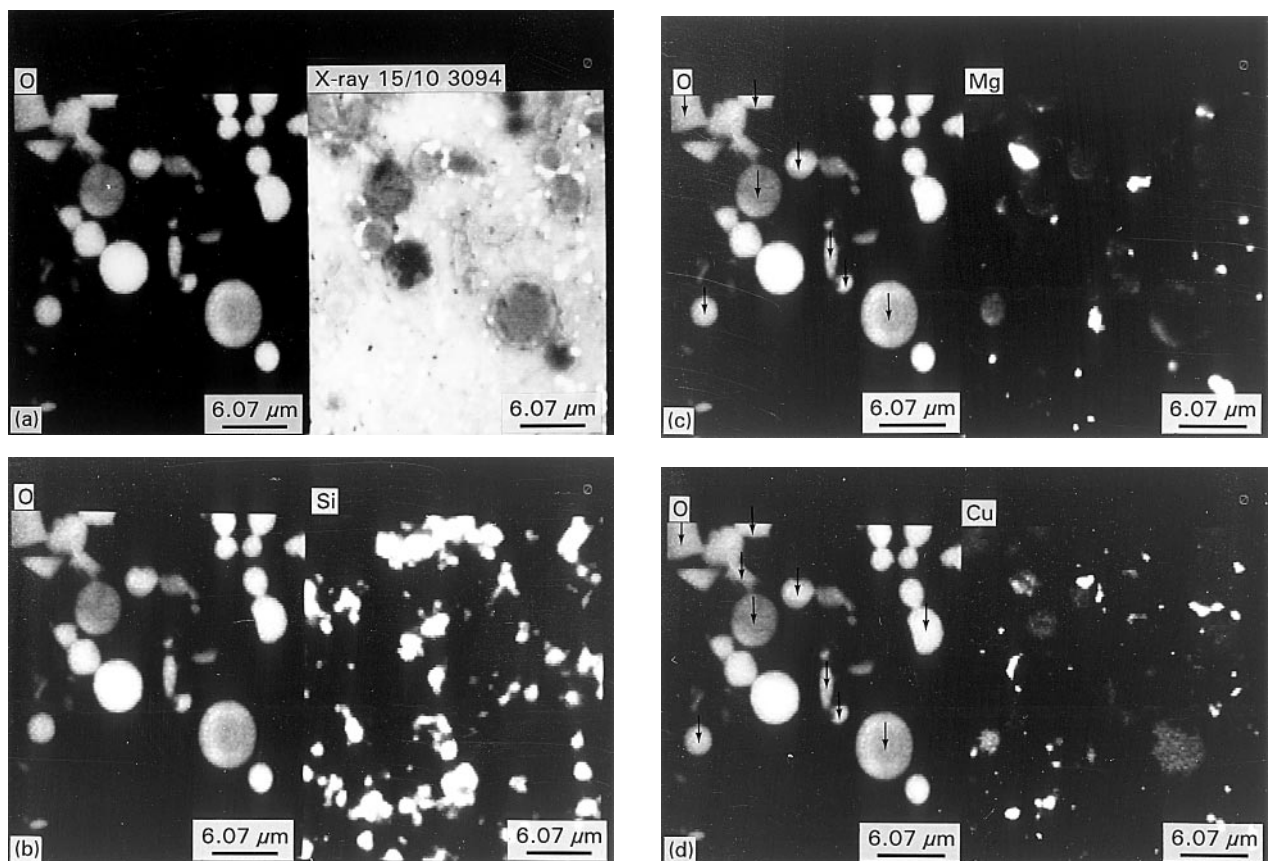


Figure 8 X-ray maps of an area in transverse cross-section of the composite with $V_f = 0.200/\text{ER } 38:1$. (a) Oxygen and the BSE image, (b) oxygen and silicon, (c) oxygen and magnesium, (d) oxygen and copper.

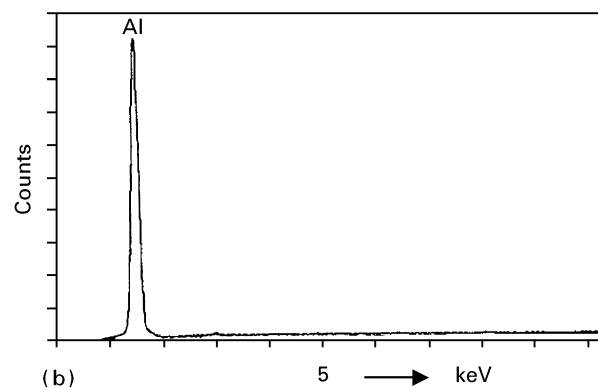
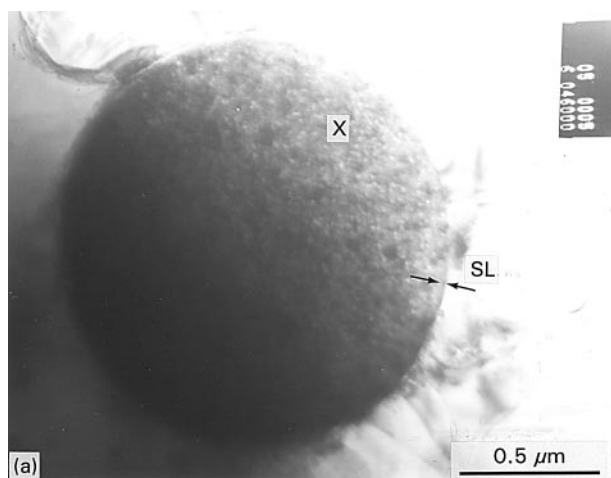


Figure 9 (a) Transmission electron micrograph of a fibre in a transverse cross-section of composite with $V_f = 0.100$ /ER 18:1; SL, dense surface layer; X, EDAX spot location. (b) EDAX spectrum of spot X in the fibre shown (a).

have a width around 10 nm, whereas the crystal domains are of a size in the range of 25–30 nm. Normally, pores are absent in an outer surface layer having a width similar to that of the crystal domains (Fig. 9). A feature of as-received fibres, similarly indicating a different texture of the outer layer and inner part, was observed by SEM (Fig. 10). Chemical probing of the fibre in Fig. 9 using the EDAX facility only revealed the presence of aluminium (Fig. 9b). Silicon particles, or the holes which they occupied because their susceptibility to argon-thinning is high, were frequently found in contact with fibres (Fig. 11a). The boundary of the fibre in this figure is rather irregular. It also lacks the continuous pore-free surface layer which is normally present. Chemical probing of the fibre gave rise to the spectrum in Fig. 11b. In addition to aluminium, copper was measured. In a number of cases where the interface constituted an apparently undisturbed (circular) boundary, copper could not be detected within the fibre. In cases of irregular fibre boundaries (Fig. 11a), copper enrichment did occur.

Although occasionally a large precipitate containing aluminium and copper was located at the fibre interface, the occurrence of precipitates in general at these locations was not widespread. In fact, fine precipitates as well as dislocations were found to be absent in a zone (of 0.25 μm) around fibres (Fig. 12).

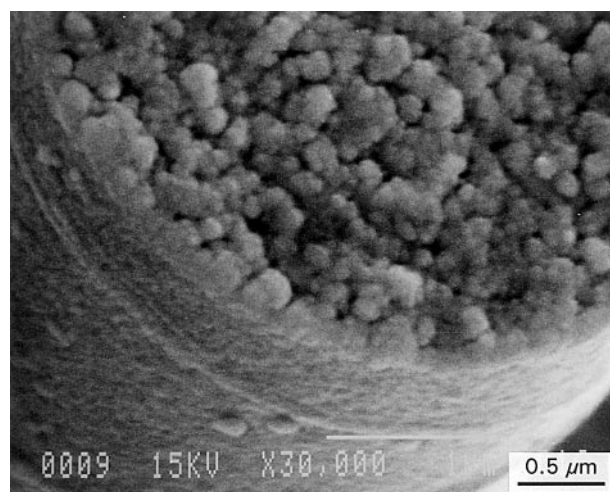


Figure 10 Scanning electron micrograph of an as-received fibre showing differences in texture between the outer fibre rim and the internal part.

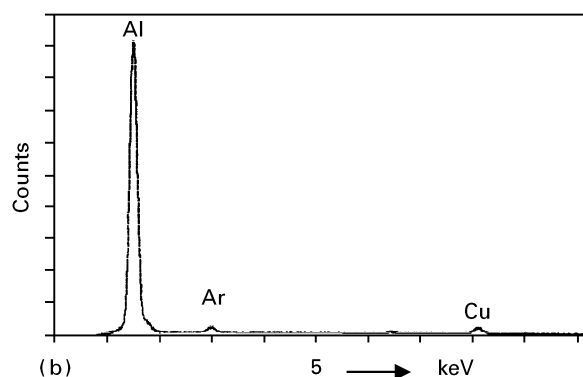
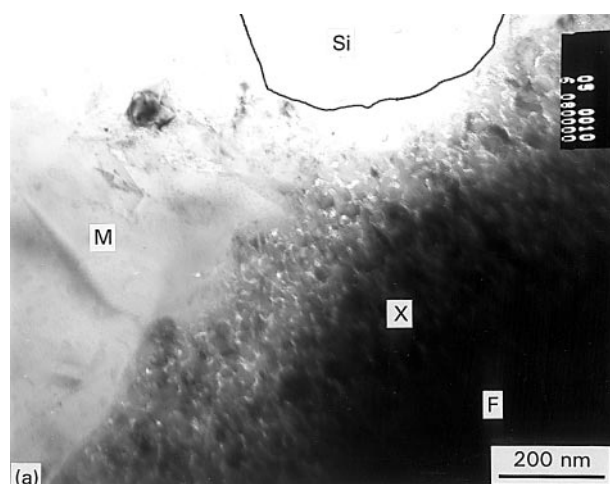


Figure 11 (a) Transmission electron micrograph of the matrix-fibre interface region in a transverse cross-section of a composite with $V_f = 0.100$ /ER 18:1; F, fibre; M, aluminium matrix; X, EDAX spot location. (b) EDAX spectrum of spot X in the fibre shown in (a).

XRD analyses were performed on fibre residues of the composites to explore the nature of the metallic enrichments in the fibre. For that, two samples were taken of composites with $V_f = 0.100$ extruded at 38:1 and 18:1. These particular materials were chosen because the former exhibited severe fibre damage and clearly contrasted with the state of fibres in the latter. The analyses revealed the presence of $\delta\text{-Al}_2\text{O}_3$ and

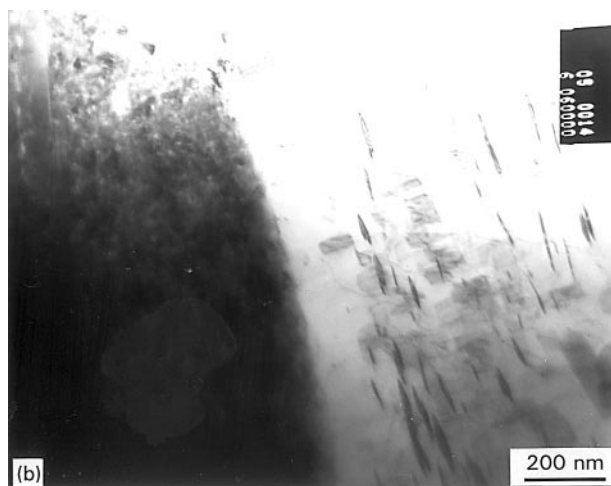
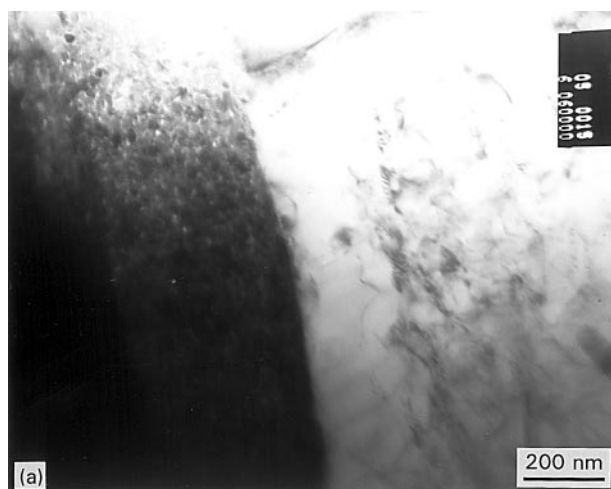


Figure 12 Transmission electron micrographs of the matrix–fibre interface region in a transverse cross-section of a composite with $V_f = 0.100/ER\ 18:1$, showing (a) dislocations and dislocation-free zone, (b) precipitates and precipitate-free zone (same area after 15° tilting).

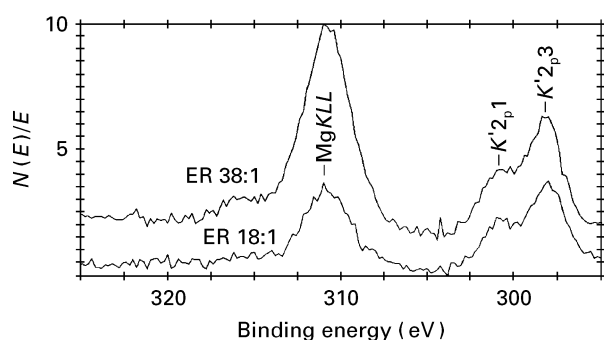


Figure 13 XPS spectra around MgKLL Auger peak showing a larger abundance of magnesium surface of fibres extracted from composite $V_f = 0.100/ER\ 38:1$, as compared to that at the surface of fibres from $V_f = 0.100/ER\ 18:1$ composite

appreciable quantities of $\alpha\text{-Al}_2\text{O}_3$ in both of the samples. Lines of magnesium- or copper-containing oxides (spinel) were not found.

Similarly extracted fibre samples (of the same materials) were subjected to semi-quantitative XPS analysis, using AlK_α radiation ($h\nu = 1486.6\text{ eV}$) at an analyser pass energy of 89.450 eV . Copper was not detected in either of the samples. The peaks from

MgKLL Auger electron excitation proved that a significant difference exists in the overall level of magnesium incorporated in the surface (Fig. 13). The absence of the Mg 1s photoelectron signal (at a binding energy of $\sim 1300\text{ eV}$) implies that the magnesium is located at depths $> 2\text{ nm}$.

4. Discussion

For the present composites, a good bonding of matrix and fibre has been reported [10].

Copper enrichment in fibres close to their damaged boundaries was observed by analytical TEM for material with $V_f = 0.100/18:1$. Fibres in this material were less impaired than those in materials extruded at a reduction ratio of 38:1. The frequency of chemically altered fibres in the latter can be expected to be significantly higher. Evidence for this may be found in the higher level of magnesium at the surface of the ER 38:1 fibres (by XPS), as compared to that at fibres of ER 18:1 material. The fact that no copper was found at the surface does not necessarily imply that it was not present: it may have been dissolved with the metallic matrix.

Evaluation of the present composites indicates that besides a size reduction (extensively described elsewhere [10]), fibres have undergone additional degradation by variable amounts of surface abrasion, cracking and chemical interaction with the matrix. These effects are especially pronounced at high reduction ratios and fibre volume fractions. The picture which emanates from the observed structural damage and chemical alteration of fibres is summarized schematically in Fig. 14. Normal cracks divide fibres into loosely attached fragments (A). Large flaws penetrate the fibre from the surface (B). Regions with a high abundance of fine flaws may be confined to the near surface (D) or extend deeply fibre inward (C, cross-hatched). Surface abrasion (D) has led to the loose, eroded fragments that were cladding fibre surfaces. It also explains the crenellated appearance of the fibre boundaries. In both stippled and cross-hatched areas, magnesium and copper enrichment may be found. In this context, it is relevant to refer to the large volume of silicon crystals of the base alloy (approximately

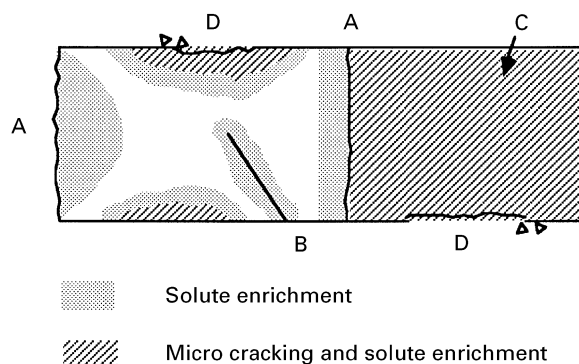


Figure 14 Schematic illustration of mechanical damage and related chemical alteration occurring in fibres. Longitudinal section. A, normal cracks; B, large flaw; C (cross-hatched), abundant microflaws and flaws; D, abraded surface with loose, eroded fragments.

20 vol %). The hardness of silicon, being 7 on the Mohs scale [12], equals that of the presently applied Saffil RF fibre [13]. Thus, mutual abrasion of these phases is feasible. In the case of high fibre volume fractions and high extrusion reduction ratios, frictional sliding between silicon particles and alumina fibres may well have led to surface abrasion damage (Fig. 14, D, see also Fig. 11a).

Previously executed nitrogen adsorption measurements pointed out that this type of δ -alumina fibre possessed a large specific surface area of $16.8 \text{ m}^2 \text{ g}^{-1}$ [14]. It was also proved that considerable porosity existed in the fibre (15 vol % [10]). Differences in texture (porosity and internal surface area) of the outer layer of the fibre and bulk were established from observations by SEM (Fig. 10) and TEM (Figs 9a and 12a).

The questions which rise in connection with the observed copper and magnesium enrichment concern (a) the chemical state in which they are incorporated, (b) the reason for their rapid diffusion, and (c) the driving force for such a (re)action. At the present stage we should like to bring to mind that the (δ)-alumina used is a metastable, so-called transition, alumina. The surfaces of these types of alumina develop catalytic properties when exposed to temperatures above 400°C at which surface hydroxyl groups are driven off [5]. These properties relate to changes in stoichiometry and involve the possibility of chemisorbing a variety of ionic species.

Strong experimental evidence supporting our expectations of an oxidized, ionic state for the metallic enrichments in the fibres is lacking. The literature suggests that the reactivity of these transition aluminas towards oxidized cationic species is higher than towards their metallic, reduced forms [16]. In an article of Wolberg and Roth [17], they reported that the formation of a CuAl_2O_4 surface phase on γ -alumina in the presence of cupric ions is possible at temperatures as low as 300°C when an appropriate alumina surface area is present. In the same article it was reported that moisture catalyses the formation of copper aluminate at the surface. At an earlier stage, they had also discovered that copper oxide dispersed at appreciable concentrations on γ -alumina (having a high specific surface area) could not be detected by XRD. The fact, therefore, that in the present extracted fibres only δ - Al_2O_3 and α - Al_2O_3 were found by XRD, does not preclude the existence of other phases: the surface of the fine porous fibre may be covered with phases which are not detected because the crystallites are too small ($< 5 \text{ nm}$ [17]).

The migration of the mentioned elements into the fibre must have taken place during extrusion. Realistically, this spans a full-constant period of 30 s at most, at temperatures between 400 and 500°C . From the field of catalyst technology, it is known that in an oxidizing atmosphere, ideal conditions occur for a solid-state reaction to occur between a metal and its oxide support [16]. Moreover, the presence of oxygen has been found to promote the diffusional bonding in some metal–alumina systems [7]. We may assume

that the partial pressure of oxygen during the present extrusion was sufficiently high to have the same effect. The reason, however, why especially copper would move out of the powder alloy into the fibre is not clear. On the other hand, a difference exists in composition between the alloy and the contacting oxide fibre, which obviously holds a thermodynamical disequilibrium and a potential driving force.

Porous transition aluminas, like the present δ - Al_2O_3 are used as carrier oxide in supported metal oxide catalysts. One of the processes leading to (undesired) deactivation of such catalysts is sintering [16], the driving force for that being (a.o.) the reduction of surface energy. It has been reported that Cu^{2+} at the surface of γ -alumina increases its sintering rate (whereas it is not modified with Mg^{2+}) [16]. The presently observed copper and magnesium enrichment of fibres could thus be the result of a sintering action. The relative large diffusional displacements, estimated to be of the order of one fibre radius, could have been covered in the short time by surface diffusion along planar fibre defects. (Diffusional supply of alloying elements to the fibre was found not to be rate-limiting.) Distances covered by diffusion along grain boundaries in all directions will have been much less. The presence of residual moisture in the composites' fibres [10] may have accelerated surface diffusion. An effect of the texture of the Saffil fibre on the diffusion distance of magnesium may be extrapolated from the work of Dinwoodie and Horsefall [2]. Incorporated in a 6061 matrix by pressure infiltration, the Saffil RF fibre showed a magnesium concentration of 1–2 wt % in an outer fibre layer of 25 nm thickness. With the use of a similar, but highly porous fibre (Saffil RG, η -alumina phase), the depth of penetration of magnesium was up to 40 times higher.

It is found that when the matrix of the present alloy is exposed to more internal parts of fibres, such as at damaged side surfaces or fibre ends, a pronounced chemical interaction can be inferred from the local enrichment of fibres with magnesium and copper. Such may have included a redox reaction, involving oxygen or water. The results indicate that the reactivity of the alloyed matrix to this type of alumina at the applied solid-state processing conditions, is essentially high. This may be the result of a complicated interaction among alloying elements and surface lattice defects of the alumina. A lack of porosity or interconnectivity of pores at the outer fibre surface, combined with a relatively low grain-boundary diffusivity, restrict a severe interaction in the case of undamaged fibres. In that case, limited chemical interaction forming a compound (oxidic) phase of a few atomic layers thickness on the external fibre surface, could possibly provide a strong bond. On the other hand, when fibres in the present composites are damaged, surface diffusion (which is more rapid than grain-boundary diffusion [18]) is allowed to occur along cracks or flaws. Combined with the high internal surface area, this may well have led to the observed amounts of copper and magnesium enrichment.

5. Conclusions

Besides fragmentation, other forms of less obvious damage are inflicted upon fibres during extrusion such as flaws, cracks and abraded surfaces. These effects, reducing the intrinsic strength of the fibre, are caused by a combination of the large volume of equally hard silicon particles and high shear strain rates (reduction ratio).

The affinity of the δ -alumina fibre to the matrix alloying elements copper and magnesium is demonstrated by analytical SEM, TEM and XPS. The relatively large extent of the interaction in some of the composites, despite the solid-state processing is a combined effect of the fibre damage, the large internal surface area and the characteristic surface properties of the transition alumina. The hypothetical chemical (redox) reaction is most severe when the matrix is exposed to internal parts of the fibre structure, i.e. at fibre ends, abraded surfaces, flaws and cracks. Parallels may be drawn with sintering mechanisms responsible for metal-oxide catalyst deactivation.

To a limited extent, the chemical reaction will also take place at the external fibre surface. It provides an answer to the good bonding behaviour of Saffil fibre and other transition alumina reinforcements to alloyed matrices, even in solid-state processing.

The presently observed mechanical and chemical degradation of fibres, most intense during extrusion of composites with high fibre volume fractions at high reduction ratios, will harm the mechanical properties of both fibre and composites.

References

1. T. W. CLYNE, M. G. BADER, G. R. CAPPLEMAN and P. A. HUBERT, *J. Mater. Sci.* **20** (1985) 85.
2. J. DINWOODIE and I. HORSFALL, in "Proceedings of Sixth ICCM and Second ECCM", edited by F. L. Matthews, N. C. R. Buskell, J. M. Hodgkinson and J. Morton (Elsevier Applied Science, London, 1987) Vol. 2.
3. R. MOLINS, J. D. BARTOUT and Y. BIENVENUE, *Mater. Sci. Eng.* **A135** (1991) 111.
4. C. G. LEVI, G. J. ABBASCHIAN and R. MEHRABIAN, *Metall. Trans* **9A** (1978) 697.
5. M. FISHKIS, *J. Mater. Sci.* **26** (1991) 2651.
6. C. R. COOK, D. I. YUN and W. H. HUNT, in "Proceedings of the International Symposium on Advances in Cast Reinforced Metal Composites", edited by S. G. Fishman and A. K. Dhingra (ASM).
7. M. G. NICHOLAS, *Mater. Sci. Forum* **29** (1988) 127.
8. G. R. CAPPLEMAN, J. F. WATTS and T. W. CLYNE, *J. Mater. Sci.* **20** (1985) 2159.
9. S. OCHIAI, T. ARAIKE, K. TOKINORI, K. OSAMURA, M. NAKATANI and K. YAMATSUTA, *ibid* **27** (1992) 4667.
10. J. H. TER HAAR and J. DUSZCZYK, *ibid.* **29** (1994) 1011.
11. *Idem*, *Mater. Sci. Eng.* **A135** (1991) 65.
12. R. C. WEAST, M. J. ASTLE and W. H. BEYER (eds), "CRC Handbook of Chemistry and Physics, 67th Edn (1986–1987).
13. Datasheet ICI, Runcorn UK.
14. J. H. TER HAAR and J. DUSZCZYK, *J. Mater. Sci.*, **28** (1993) 3103.
15. K. WEFERS and C. MISRA, Alcoa Technical Paper 19; "Oxides and Hydroxides of Aluminium" (Alcoa Laboratories, 1987).
16. B. DELMON and P. GRANGE, in "Catalyst Deactivation, Proceedings of the International Symposium," edited by B. Delmon and G.F. Froment (Elsevier Scientific, Amsterdam, 1980) p. 507.
17. A. WOLBERG and J. F. ROTH, *J. Catal.* **15** (1969) 250.
18. J. NOWOTNY, *Mater. Sci. Forum.* **29** (1988) 99.

Received 2 March 1994

and accepted 24 May 1995